INTERNATIONAL JOURNAL OF CURRENT RESEARCH IN CHEMISTRY AND PHARMACEUTICAL SCIENCES
(p-ISSN: 2348-5213: e-ISSN: 2348-5221)
www.ijcrcps.com
Coden: IJCROO(USA) Volume 3, Issue 4 - 2016
Research Article
SOI: http://s-o-i.org/1.15/ijcrcps-2016-3-4-5

EVIDENCES OF DRUG ACTIVITY OF CYCLOSERINE THROUGH EXPERIMENTAL AND SIMULATED THEORETICAL MODELS

M MANIVANNAN*, B KARTHIKEYAN, K RAJESHWARAN
Department of Chemistry, Annamalai University, Annamalainagar, 608002
*Corresponding Author: mani080871@gmail.com

ABSTRACT

4-Amino-3-isoxazolidinone (or) R-(+)-Cycloserine, **Figure-I**, emerged as an anti-tuberculosis drug [1][2], sold under the brand name Seromycin and now it is in the World Health Organization's list of essential medicines needed in a basic health system. This unusual amino acid derivative gained much interest from the physical chemists, in recent past, in view point of its electronic structure and its conformational stability [3]. For the treatment of tuberculosis, R-(+)-Cycloserine is classified as a second-line drug [4][5]. Treating children with obsessive compulsion disorder with R-(+)-Cycloserine has been investigated recently and also been used in the clinical trials against Alzheimer's disease. By considering the importance of this compound and to put light on its industrial preparations and validation of analytical methods, we have reinvestigated 1H and 13C NMR, FT-IR, Achiral HPLC and mass spectrometry along with density functional theoretical (DFT) methods. For the first time, the Raman spectrum of the title compound has been simulated and Drug-Docking studies have been attempted. The forbidden energy gap between its frontier molecular orbitals, viz. HOMO-LUMO were calculated and correlated with its photo-stability. The molecular electrostatic potential diagram is also been mapped to explain the chemical activity. Based on the results, a mechanism of its drug-action through its active chiral centre has been proposed.

KEYWORDS: Cycloserine, Anti-tuberculosis, Seromycin, Raman spectra, HPLC etc.

1. INTRODUCTION

4-Amino-3-isoxazolidinone (or) R-(+)-Cycloserine, **Figure-I**, emerged as an anti-tuberculosis drug, sold under the brand name Seromycin and now it is in the World Health Organization's list of essential medicines needed in a basic health system. This unusual amino acid derivative gained much interest from the physical chemists, in recent past, in view point of its electronic structure and its conformational stability. For the treatment of tuberculosis, R-(+)-Cycloserine is classified as a second-line drug, i.e. its use is only considered if one or more first-line drug cannot be used. In other words, it is very effective against multi-drug resistant strains of Mycobacterium Tuberculosis. Another reason for its limited use is the adverse neurological side effects it causes, since it can easily penetrate into the central nervous system (CNS).

Oxazolidinone, the parent compound of R-(+)-Cycloserine was investigated extensively by theoretical and Photo-electron spectroscopic studies [6]. Treating childrens with obsessive compulsion disorder with R-(+)-Cycloserine has been investigated recently [7] and certain genito-urinary infections caused by Enterobacteria (or) E-coli [8][9]. For past few years, it has also been used in the clinical trials against Alzheimer's disease [10].

For the first time, the Raman spectrum of the title compound has been simulated and Drug-Docking studies have been attempted. The molecular electrostatic potential diagram is also been mapped to explain the chemical activity. Based on the results, a mechanism of its drug-action through its active chiral centre has been proposed.

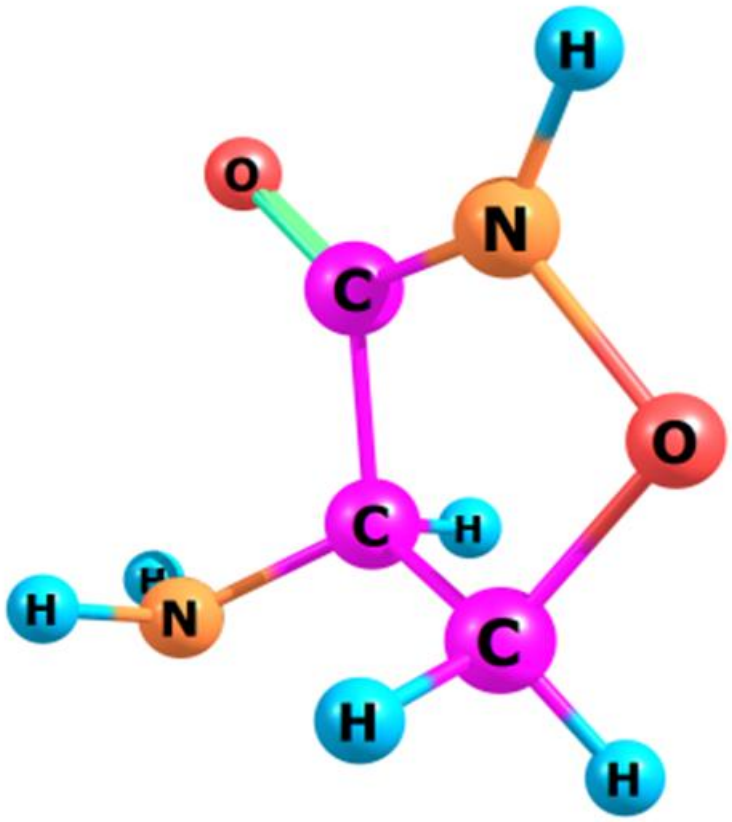

FIGURE: I- Optimized structure of R-(+)-Cycloserine

2. EXPERIMENTAL SECTION

2.1 CHEMICALS USED

All chemicals and reagents used were of analytical grade (AR) and used as received. Sodium 1-decanesulfonate, Sodium hydroxide, Potassium phosphate monobasic and Acetonitrile were purchased from Sigma-Aldrich. De-ionized water was used in all the experiments and the glassware were cleaned and dried in a hot air oven at ≥ 100˚C.

2.2 MASS SPECTROMETRY

Mass spectra were recorded on the **SHIMADZU GC-MS** system, involving electron ionization technique for fragmentation by an accelerated electron of energy of about ~70 MeV.

2.3 IR SPECTRA

The FT-IR spectra were recorded in **PERKIN ELMER SPECTRUM ONE FT-IR** spectrometer by mixing about 1-2 mg of the analyte with 300-400 mg of finely powdered KBr and the scan range was maintained within 10 % between the sample and the reference.

2.4 1H NMR SPECTRA

The 1H NMR spectra of Cycloserine were recorded in **BRUKER 300 MHz Avance NMR** spectrometer using TMS as an internal standard owing its precessing resonance frequency with the applied Radio-wave frequency at 0 ppm in δ-scale (the chemical shift value). Furthermore, the sampling of analyte was done by employing highly polar solvent, D2O (heavy water).

2.4 13C NMR SPECTRA

The proton decoupled 13C NMR spectra were recorded on BRUKER 300 MHz, with operating frequency of about 75 MHz, Avance NMR spectrometer, by using deuterated Dimethyl sulfoxide(DMSO) as a solvent. TMS was used as an internal standard.

2.5 HIGH-PERFOMANCE LIQUID CHROMATOGRAPHY (ACHIRAL)

The HPLC instrumentation technique was employed with non-reciprocating pump and sample injection system all together connected in a series with **WATERS-2414 Refractive index (RI)** detector and controlled by **EMPOWER-II** software version 6.10.00.000. The Solvent delivery system was flow programming in which the flow rate of a constant composition (Isocratic) mobile phase was increased during the run.All the reagents and chemicals utilized were of analytical grade (AR). Acetonitrile and water were of HPLC grade.

2.5.1 MOBILE PHASE

The mobile phase was comprised of 0.5 g of Sodium 1-decane sulfonate in 800 ml of water having acidic buffer of acetonitrile and glacial acetic acid and made adjusted to pH of 4.4 by using caustic soda. Finally, the mobile phase was filtered with 0.2µ filter paper and degassed before running the chromatogram.

2.5.2 CHROMATOGRAPHIC CONDITIONS

Column dimension : 1250 m.m×4.6 m.m×5 µ
Column model : ZORBAX ODS C18
Oven temperature : 30·C
Mobile phase : Isocratic
Injection volume : 40 µL
Flow rate : 1.0 ml/min
Wavelength : 219 nm
Diluent : Potassium phosphate monobasic (0.2 M) and Sodium hydroxide (0.2 M) in 2:1 ratio.

2.6 THEORETICAL METHOD

Density functional theoretical (DFT) calculations were performed using Gaussian-03 [11] program package on a Pentium IV processor personal computer without any constraint on the geometry. The BECKE 3LYP hybrid functional has been used throughout the work. It consisted of the non-local exchange functional of BECKE'S [12] three parameter set and the non-local correlation functional of Lee, Yang and Parr [13]. The 6-31G (d) basis set had been invoked in the calculations. Harmonic vibrational analyses have been done to determine the stationary point as minima at DFT level. Finally the calculated normal modes of vibrational frequencies provided the thermodynamic properties by using statistical model and also to support the vibrational assignments and to ascertain the nature of functional groups present in the experimental FT-IR and NMR spectra of the title compound.

3. RESULTS AND DISCUSSION

3.1 MASS SPECTROMETRY

The mass spectrum of the title compound is given in **Figure 3.1** and the obtained experimental data were given in the **Table 3.1.**

TABLE: 3.1 Mass spectral peaks and possible fragmentations

m/z Value	Possible fragmented Ions
102	[M]+
103	[M+1]+
43	[HN-C=O]+
30	[NO]+

[M]+,the molecular ion.

The observed low intensity peak at m/z=102 corresponds to the molecular ion [M]+, having the molecular formula **C3H6N2O2**, and the[M]+ ion peak is accompanied by[M+1]+ion peak because of a small fractions of 13C isotope inevitably present in the sample in the ratio of 100:1.1. The intense peak at m/z=43, so called base peak, is observed and most probably due to the daughter ion [HN-C=O]+ , which is favoured by resonance and thermodynamic conditions.

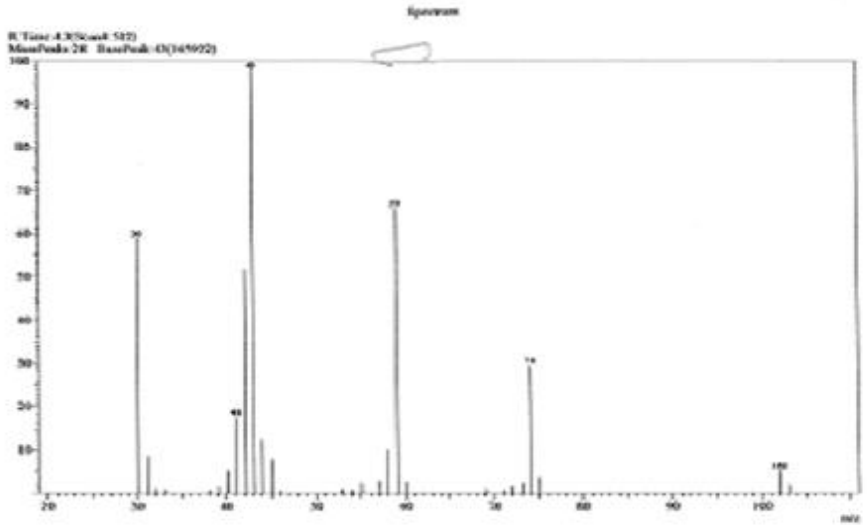

FIGURE: 3.1 Mass spectrum of cycloserine

Similarly, the peak at m/z=30 is corresponds to the sub-fragment ion [NO]+ with a relative abundance of 60%. Furthermore, the two mass peaks with considerable relative abundance at m/z=74 and 59 could be probably due to the fragment loss of [CO] + and [HN-C=O] + ions from the molecular ion, respectively.

3.2 IR SPECTRAL ANALYSIS

The FT-IR spectrum of 4-Amino-isoxazolidin-3-one (Cycloserine) is given in the **Figure 3.2** and the prominent vibrational frequencies are given in the following **Table 3.2**

Wave number (cm-1)	Assignment
959.53	C-O-N In-plane Bending vibration
1367.38	CH2 Bending vibration
1416.62	NH Bending vibration
1463.96	
1561.80	CH2 In plane Bending vibration
1686.55	C=O Asym. stretching vibration
2874.13	C-H Symmetric stretching vibration
2931.71	C*-H Asym. stretching vibration
3117.70	
3387.84	NH2 Asymmetric stretching vibration
3840.33	NH Asymmetric stretching vibration

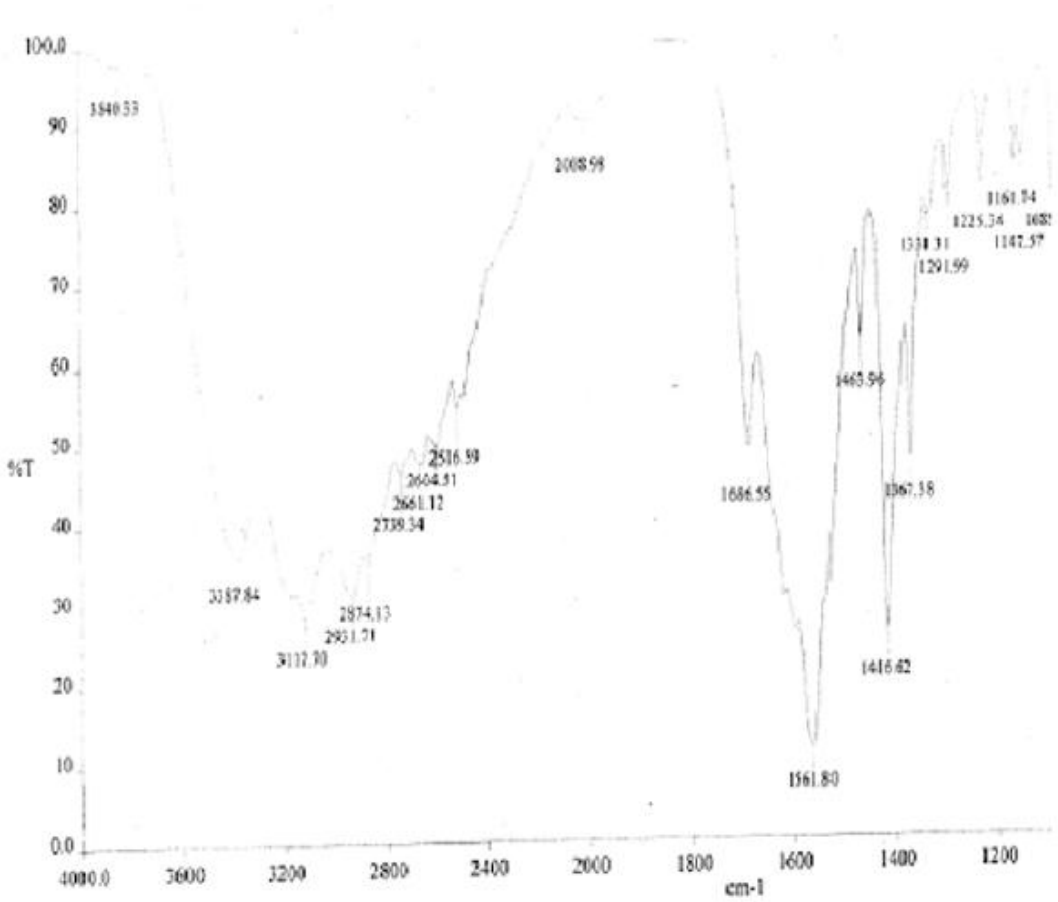

FIGURE: 3.2 FT-IR spectrum of cycloserin

An intense IR vibrational frequency is observed at 1686.55 cm**-1** which corresponds to the asymmetric stretching vibrational mode of carbonyl group of amidic moiety present in the molecule. A slightly less intense

peak at 1463.96 cm**-1** and much intense peak at 1561.80 cm**-1** belong to the bending, most probably scissoring vibrational mode of CH2 and NH2 groups respectively [14].

Similarly, the CH and NH symmetric stretching was observed at 2874.13 and 3840.33 cm**-1** respectively [15]. The experimental IR spectrum was correlated with the theoretical IR spectral data which was obtained from the density functional theoretical calculations, to ascertain the nature of functional groups present in the title molecule.

THEORETICAL STUDIES ON CYCLOSERINE

3.3 OPTIMIZED MOLECULAR GEOMETRY

The labeling and bond lengths between various atoms of Cycloserine are given in the **Figures 3.3** and **3.4**. The optimized geometrical parameters have been listed in the **Table 3.2**. The theoretical model showed consistent optimized bond parameters.

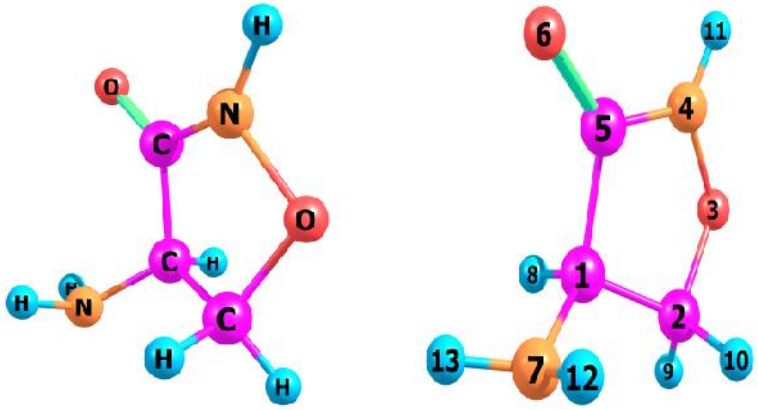

FIGURE: 3.3 Optimized molecular geometry

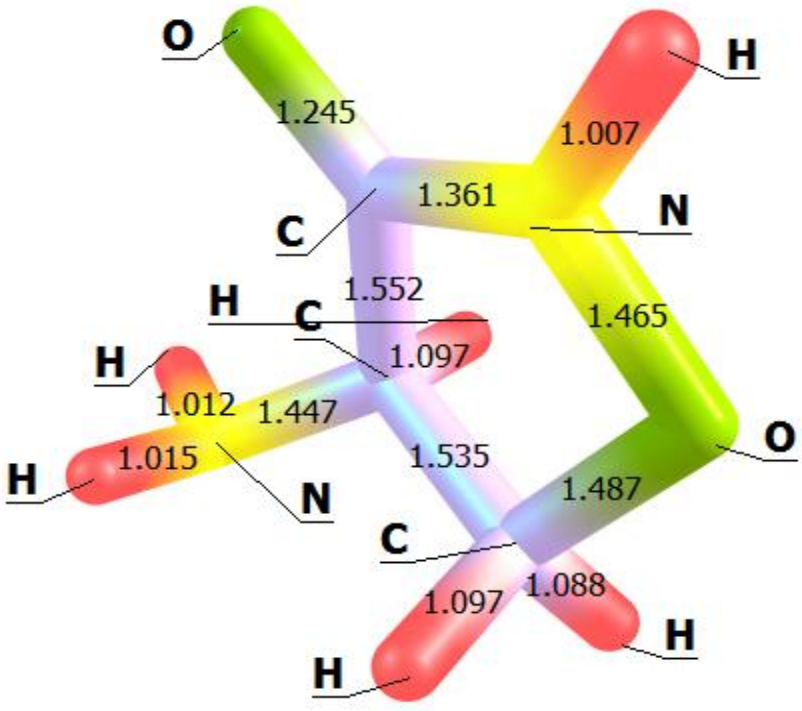

FIGURE: 3.4 Optimized geometry with bond lengths

TABLE: 3.2 Optimized geometrical parameters of Cycloserine

Parameters	Obtained values Å/Degree	Parameters	Obtained values Degree/ υ	Parameters	Obtained values Degree/ υ
R(1-2)	1.535	A(1-7-12)	114.6	W12(A)	807.4
R(1-5)	1.552	A(1-7-13)	114.4	W13(A)	879.0
R(1-7)	1.447	A(3-2-9)	106.0	W14(A)	979.0
R(1-8)	1.097	A(3-2-10)	109.4	W15(A)	1009.4
R(2-3)	1.447	A(2-3-4)	102.4	W16(A)	1034.2
R(2-9)	1.097	A(9-2-10)	110.6	W17(A)	1178.3
R(2-10)	1.487	A(3-4-5)	113.4	W18(A)	1197.3
R(3-4)	1.088	A(3-4-11)	113.9	W19(A)	1251.3
R(4-5)	1.097	A(5-4-11)	130.5	W20(A)	1272.9
R(4-11)	1.465	A(4-5-6)	126.7	W21(A)	1312.3
R(5-6)	1.361	A(12-7-13)	111.6	W22(A)	1361.1
R(7-12)	1.007	A(1-7-12)	114.6	W23(A)	1380.2
R(7-13)	1.245	A(1-7-13)	114.4	W24(A)	1435.6
A(2-1-5)	1.015	W1(A)	107.9	W25(A)	1531.5
A(2-1-7)	1.012	W2(A)	190.5	W26(A)	1721.3
A(2-1-8)	102.3	W3(A)	218.6	W27(A)	1735.3
A(1-2-3)	113.2	W4(A)	257.7	W28(A)	3062.8
A(1-2-9)	110.2	W5(A)	359.9	W29(A)	3077.2
A(1-2-10)	104.7	W6(A)	440.5	W30(A)	3187.1
A(5-1-7)	115.0	W7(A)	487.7	W31(A)	3539.6
A(5-1-8)	110.8	W8(A)	595.7	W32(A)	3657.0
A(1-5-4)	115.7	W9(A)	680.4	W33(A)	3688.3
A(1-5-6)	126.7	W10(A)	682.6	-	-
A(7-1-8)	108.2	W11(A)	698.6	-	-

R– Bond length, A – Bond angle and W–Vib.Frequencies

.

The optimized molecular geometry of Cycloserine clearly shows typical bond length parameters between the respective atoms, Viz. σ-C2 (sp3)- C3 (sp3)=1.5352Å , σ-C6 (sp3)- C2 (sp2)=1.552 Å, σ-(C2-N1)=1.447Å and (C=O) is 1.245Å [16]. Except that of the bond length parameter between the N-atom at position- 4 and the C-atom at position- 5 and is about 1.361 Å which is considerably much lesser than the expected C-N bond length of about 1.4 Å -1.5 Å. Interestingly it is much closer to that of the partial double-bond character observed in pyridine i.e. in pyridine the C-N bond length is only about 1.35 Å possess partial double bond character due to resonance delocalization of closed loop of pi-electrons [17]. The electron-deficient C-atom, at position- 5, of highly polar carbonyl group of cycloserine can attracts the lone pair of electrons on the N-atom at position- 4 and it may causes the partial double-bond character of the C-N bond between positions- 4 & 5. The existence of H-bonding or any other electronic effects such as tautomerism etc are ceases to exist in the gaseous phase of molecules. Furthermore, the calculated atom-atom bond order, **Table 3.3**, shows a unusual bond order of about 1.084 which is more for the C-N σ-bond. This also suggests the existence of a partial double-bond character between the C and N at positions- 5 and 4, respectively.

3.3.1 VIBRATIONAL ASSIGNMENTS

R-(+)-Cycloserine, a non-linear planar molecule possesses C1 point group symmetry. The molecule has 13 atoms and 33 normal modes of fundamental vibrations [18]. All the 33 vibrations were active in both IR and Raman. The harmonic vibrational frequencies calculated for Cycloserine at B3LYP level using the triple split valence basis set along with diffuse and polarization functions, 6-31G (d) have been presented in **Table 3.4**. Comparison of the frequencies calculated at B3LYP with experimental assignments (**Table 3.4**) revealed that the over estimation of the calculated vibrational modes arises due to neglecting inherent anharmonicity of the real system.

Hence, it is customary to scaling down the calculated harmonic frequencies in order to achieve a reasonable agreement between an observed and theoretically obtained value [19]. For DFT calculations utilizing the Becke's three parameter LYP 6-31G (d) basis set, the optimal scaling factor of about 0.9613 has been used to eliminate known systematic errors in computed frequency. The scaled down values were also given in the **Table 3.5**. The computed IR and Raman spectra of Cycloserine at B3LYP level using 6-31G (d) have been shown in **Figures 3.5 and 3.6.**

TABLE: 3.3 Wieberg atom-atom bond orders

	1	2	3	4	5	6	7	8	9	10	11	12	13
1	0.000000												
2	0.963396	0.000000											
3	0.010724	0.961130	0.000000										
4	0.034708	0.008418	0.967933	0.000000									
5	0.910827	0.011136	0.026672	1.084481	0.000000								
6	0.046253	0.008477	0.020296	0.159756	1.754046	0.000000							
7	1.002260	0.005911	0.003743	0.007126	0.023038	0.009777	0.000000						
8	0.935066	0.003131	0.001329	0.006018	0.006556	0.005860	0.003042	0.000000					
9	0.003293	0.953492	0.009201	0.006631	0.002774	0.000394	0.001987	0.000808	0.000000				
10	0.006302	0.953143	0.014837	0.000958	0.000619	0.000282	0.002449	0.004383	0.005189	0.000000			
11	0.011494	0.005504	0.019068	0.849099	0.017461	0.012537	0.002082	0.000219	0.000840	0.000008	0.000000		
12	0.002890	0.000144	0.000007	0.000348	0.002197	0.000496	0.968490	0.009552	0.000001	0.000651	0.000089	0.000000	
13	0.002126	0.010615	0.000916	0.000278	0.001197	0.001102	0.962505	0.000040	0.000380	0.000014	0.000020	0.000614	0.000000

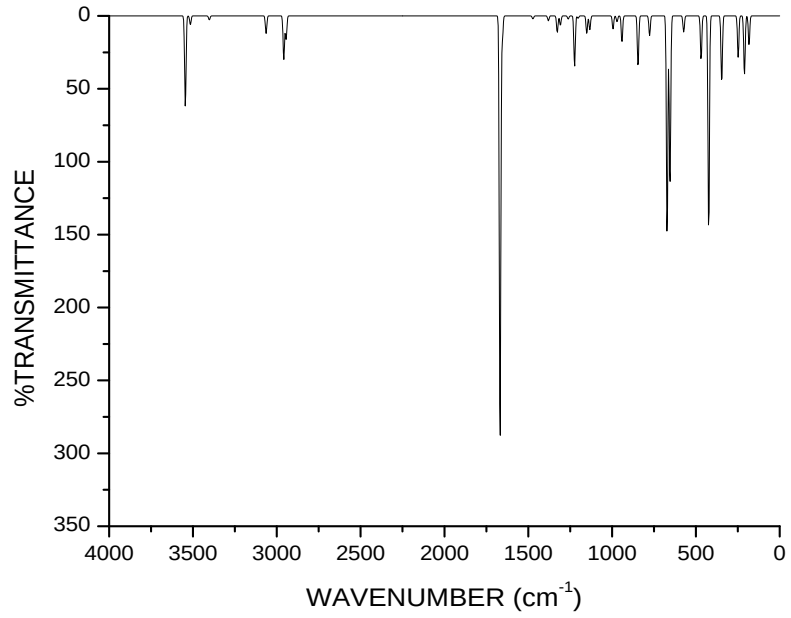

FIGURE: 3.5 Computed IR spectrum of cycloserine

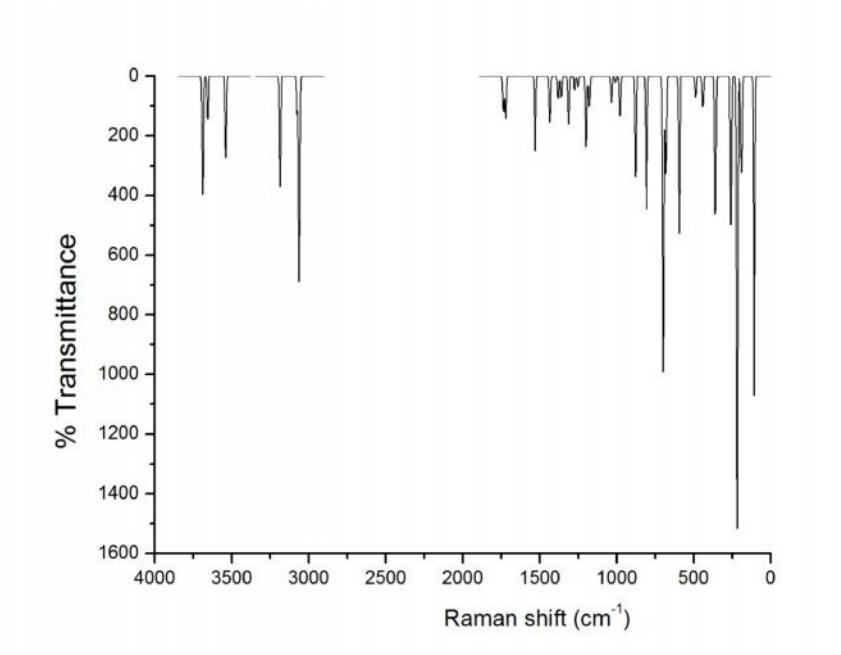

FIGURE: 3.6 Computed Raman spectrum of cycloserine

TABLE: 3.4 Vibrational wave numbers computed for Cycloserine at B3LYP/6-31G(d) method

S. No.	Calculated vibrational frequencies (cm-1)	Calculated IR Intensity	Calculated RAMAN Intensity	Experimental IR (cm-1)	Assignments
1.	107.90	0.03	1093.57		CO-CH bending vibration
2.	190.46	19.65	322.87		N-O-C out of plane bending
3.	218.56	40.84	1562.49		NH2 out of plane bending
4.	257.68	28.36	498.63		C-NH2 bending vibration
5.	359.91	46.43	496.26		NH out of plane bending
6.	440.51	149.73	107.15		NH out of plane bending
7.	487.70	30.02	71.46	509.56 W	NH out of plane bending
8.	595.70	11.07	528.78	594.97 W	C-C-C in-plane bending
9.	680.36	97.01	101.19		N-CO-C out of plane bending
10.	682.62	23.41	241.16		O-N out of plane bending
11.	698.60	151.27	1019.05	701.42 W	NH2 out of plane bending
12.	807.42	13.59	451.37	815.51 W	CO-C bending vibration
13.	878.97	35.15	356.57	888.12 M	C-O asym. Stretching
14.	979.04	18.64	142.61	959.53 M	C-O-N in-plane bending
15.	1009.40	4.12	20.66	997.39 W	C-C-C ring bending
16.	1034.23	8.92	88.71	1085.81 W	C-C ring bending
17.	1178.28	9.47	99.98	1147.57 W	CH2 out of plane bending
18.	1197.29	12.30	245.12		CH2 bending
19.	1251.32	1.69	34.50		NH2 in-plane bending
20.	1272.88	35.00	45.83	1291.99 W	NH in-plane bending
21.	1312.29	2.18	160.11		C*-H in-plane bending
22.	1361.08	6.52	73.56	1367.38 M	CH2 in-plane bending
23.	1380.19	11.44	76.30	1416.62 M	NH bending
24.	1435.56	3.38	156.19	1463.96 W	C*-H out of plane bending
25.	1531.45	2.07	270.08	1561.80 S	CH2 in-plane bending
26.	1721.34	16.87	143.36		NH2 in-plane bending
27.	1735.28	298.65	121.63	1686.55 S	CO asym. Stretching
28.	3062.80	16.00	690.36	2874.13 S	CH symmetric stretching
29.	3077.20	30.04	124.88	2931.71 S	C*-H asym. Stretching
30.	3187.05	12.05	371.49	3117.70 S	C-C asymmetric stretching
31.	3539.55	2.77	281.87	3387.84 W	NH2 asym. Stretching
32.	3657.04	6.115	151.84		NH2 asymmetric stretching
33.	3688.30	62.93	405.96	3840.33 W	NH asymmetric stretching

W – weak; M – medium; S – strong.

The vibrational assignments are carried out by Gauss view program software [20] and compared with the literature data of similar molecules.

TABLE: 3.5 Comparison between theTheoretical and experimental vibrational frequencies of Cycloserine

S. No.	Calculated vibrational frequencies (cm-1)		Experimental IR (cm-1)	Assignment
	before scaling	after scaling		
1.	107.90	103.72		CO-CH bending vibration
2.	190.46	183.09		N-O-C out of plane bending
3.	218.56	210.10		NH2 out of plane bending
4.	257.68	247.71		C-NH2 bending vibration
5.	359.91	345.98		NH out of plane bending
6.	440.51	423.46		NH out of plane bending
7.	487.70	468.83	509.56 W	NH out of plane bending
8.	595.70	572.65	594.97 W	C-C-C in-plane bending
9.	680.36	654.03		N-CO-C out of plane bending
10.	682.62	656.20		O-N out of plane bending
11.	698.60	671.56	701.42 W	NH2 out of plane bending
12.	807.42	776.17	815.51 W	CO-C bending vibration
13.	878.97	844.95	888.12 M	C-O asym. Stretching
14.	979.04	941.15	959.53 M	C-O-N in-plane bending
15.	1009.40	970.34	997.39 W	C-C-C ring bending
16.	1034.23	994.21	1085.81 W	C-C ring bending
17.	1178.28	1132.68	1147.57 W	CH2 out of plane bending
18.	1197.29	1150.95		CH2 bending
19.	1251.32	1202.89		NH2 in-plane bending
20.	1272.88	1223.62	1291.99 W	NH in-plane bending
21.	1312.29	1261.50		C*-H in-plane bending
22.	1361.08	1308.40		CH2 in-plane bending
23.	1380.19	1326.78	1416.62 M	NH bending
24.	1435.56	1380.00	1463.96 W	C*-H out of plane bending
25.	1531.45	1472.19	1561.80 S	CH2 in-plane bending
26.	1721.34	1654.72		NH2 in-plane bending
27.	1735.28	1668.13	1686.55 S	CO asym. Stretching
28.	3062.80	2944.26	2874.13 S	CH symmetric stretching
29.	3077.20	2958.11	2931.71 S	C*-H asym. Stretching
30.	3187.05	3063.71	3117.70 S	C-C asymmetric stretching
31.	3539.55	3402.57	3387.84 W	NH2 asym. Stretching
32.	3657.04	3515.52		NH2 asymmetric stretching
33.	3688.30	3545.57	3840.33 W	NH asymmetric stretching

W –weak; M – medium; S – strong.

3.3.2 THERMOCHEMICAL STUDIES OF CYCLOSERINE

In DFT calculations**,** all frequency assignments were accompanied by the thermo-chemical analysis of the system viz., Thermal energy includes a scaled zero point energy or thermal energy corrections, the heat capacity at constant volume, entropy of the system etc., at 298.15K and at 1 atm. The calculated values are given in the **Table 3.6**. The HF energy limit is found to be -377.68 Hartrees per particle and the heat of formation is calculated to be -13.780 kcal/mol.

TABLE: 3.6 Thermochemical data of cycloserine

TOTAL ENERGY	**E** (Thermal) (kcal/mol)	**CV** (Cal/mol-K)	**S** (Cal/mol-K)
	68.657	24.779	81.600
Electronic	00.000	00.000	00.000
Rotational	00.889	2.981	27.206
Translational	00.889	2.981	39.778
Vibrational	66.880	18.817	14.116

The total energy of the system is given by the sum of the electronic energy and the thermal energy of the system, at 298.150 K and 1 atm, including the zero-point energy correction

3.3.3 FRONTIER MOLECULAR ORBITALS

In cycloserine, there are 40 valence electrons constituting the molecular orbitals in which the highest occupied molecular orbital (HOMO), with anti-symmetric properties, having energy of about -6.259 e V and the lowest unoccupied molecular orbital (LUMO) with energy of about 0.123 e V.

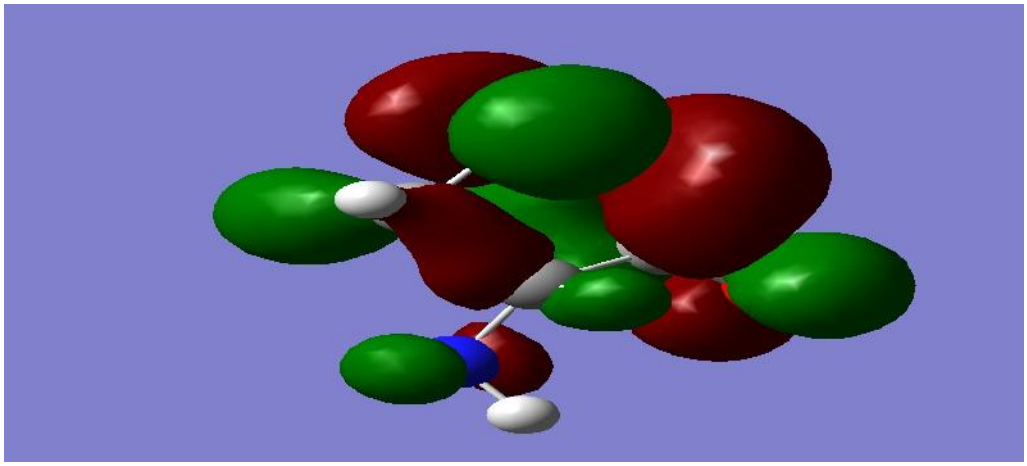

FIGURE: 3.7 HOMO of cycloserine

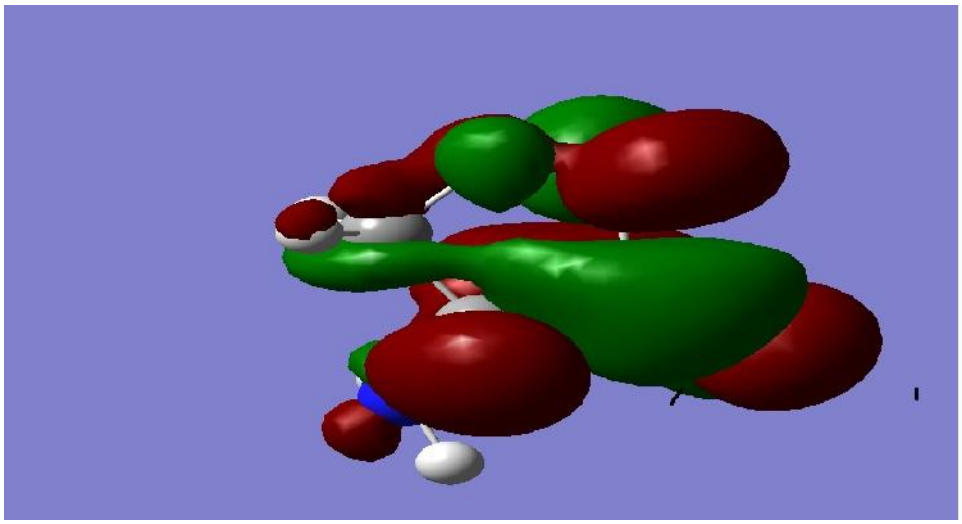

FIGURE: 3.8 LUMO of cycloserine

The energy gap or excitation energy between those frontier molecular orbitals is calculated to be 6.381e V and shown in the **Figure 3.9**

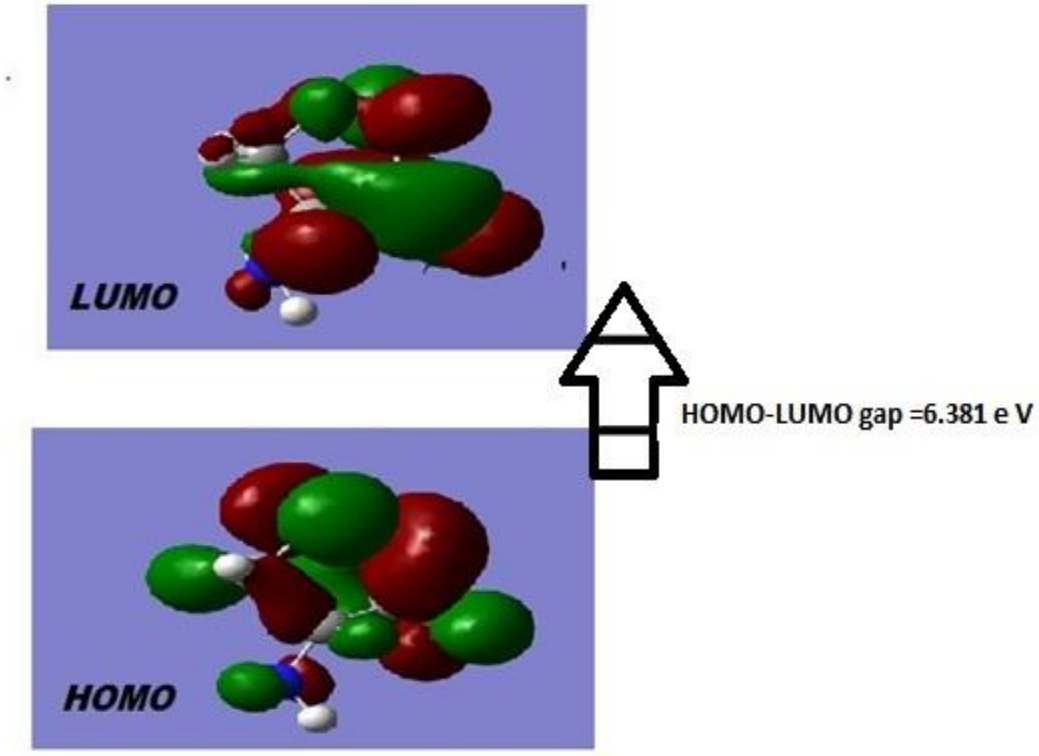

FIGURE: 3.9 Energy gap between frontier molecular orbitals

3.3.4 DIPOLE MOMENT AND MULLIKEN ATOMIC CHARGES

The dipole moment of cycloserine is found to be 1.6769 D and the respective dipole moment vector components along the Cartesian co-ordinates is shown in the **Table 3.7**. The overall dipole moment value is nearly equivalent to that of water, **μ**H2O =1.85 D. In other words, the cycloserine molecule is highly polar in nature and can easily soluble in polar solvents unlike other non-polar organic compounds.

TABLE: 3.7 Electric dipole moments and dipole moment components of cycloserine

DIPOLE VECTOR COMPONENTS	DIPOLE MOMENT μ (DEBYE)	
	Cycloserine	water
μx	-0.5865	-
μy	-1.5625	-
μz	-0.1632	-
μTotal	1.6769	1.85

Furthermore, the acidic protons on the molecule are labile and can easily ex-changeable in a suitable conditions [21]. This is also well supported by the 1H NMR spectrum of the compound in deuterated solvent molecules.

The calculated Mulliken atomic charges involve the electron affinity values of the respective atoms in the molecules. For cycloserine, the Mulliken charges at restricted Hartree-Fock B3LYP 6-31G (d) model level is given in the **Table 3.8** as well as in the **Figure 3.9.**.

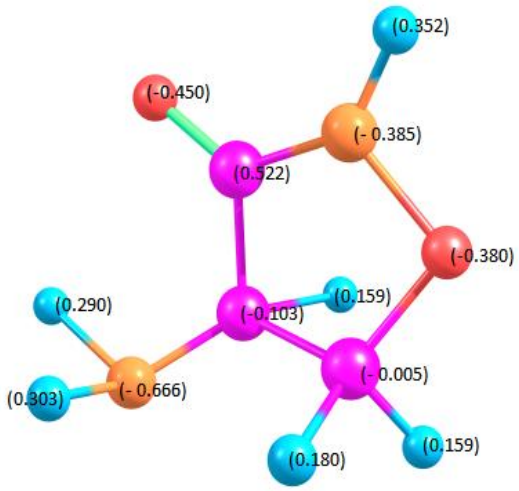

FIGURE: 3.9.1 Cycloserine with calculated Mulliken's charge

TABLE: 3.8 Mulliken's atomic charges on cycloserine

POSITIONS	ATOMS	CHARGE
1	C*	-0.103
2	C	-0.005
3	O	-0.380
4	N	-0.385
5	C	0.522
6	O	-0.450
7	N	-0.666
8	H	0.183
9	H	0.159
10	H	0.180
11	H	0.352
12	H	0.303
13	H	0.290

3.3.5 MOLECULAR ELECTROSTATIC POTENTIAL (MEP)

The molecular electrostatic potential diagram generally represents the probability of electron density integrated over the entire space around the system or molecule. It will provide versatile information about the reactive sites, viz. the electrophilic and nucleophilic centers in the molecular system available for the chemical as well as bio-chemical processes [22], H-bonding's [23], dipole-dipole interactions etc. The electrostatic potential of the title compound is depicted in the **Figure 3.8**.

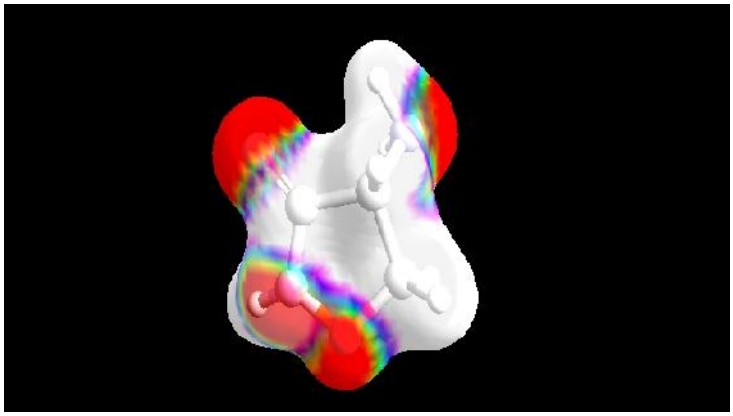

FIGURE: 3.9.2 Molecular electrostatic potential diagram of cycloserine

The MEP diagram representing the time in-variant electric field charges on Cycloserine reveals the most active reactive sites, the electron-rich densities, at positions-1,4,5 and 6 corresponds to the N-atom of primary (1º) amine, ethereal O-atom, the N-atom on 2ºamine and the carbonyl group, respectively. This explains the hydrolysis of cycloserine to D-serine and Hydroxylamine [24].

3.4 1H NMR SPECTRUM OF CYCLOSERINE

The obtained experimental 1H NMR spectral data is shown in the following **Table 3.8** and in the **Figure 3.9.3**,

TABLE: 3.8 1H NMR experimental spectral data of cycloserine

Position	δ-Value (ppm)	Multiplicity
4	4.29 - 4.34	One H Triplet
5	4.18 - 4.23	One H(a) doublet of doublet
	4.51 - 4.57	One H(b) doublet of doublet

The 1H NMR spectrum of the title molecule clearly revealed a sharp triplet at 4.31 ppm which corresponds to a methine proton at position-4, having vicinal spin – spin coupling with the two methylene protons at position-5. Similarly, the two doublet of doublet at 4.18 ppm and 4.51 ppm corresponds to the two geminal protons residing at the methylene C-atom at position-5. The two diastereotopic methylene protons at position-5 became magnetically different to one another with the chemical environment which accounted for the observed peaks viz., a doublet for each methylene protons at position-5. Apart from the spin-spin coupling, the two diastereotopic protons at position-5, experiences de-shielding effect from the more electronegative O-atom at adjacent position. Consequently, the δ-value shifted towards downfield region, when compared to the methylene protons having no such de-shielding at all. Importantly, an intense and sharp singlet at 4.8 ppm attributed to the protons of solvent molecules, H-OD , produced due to the isotopic-exchange reaction between D2O and

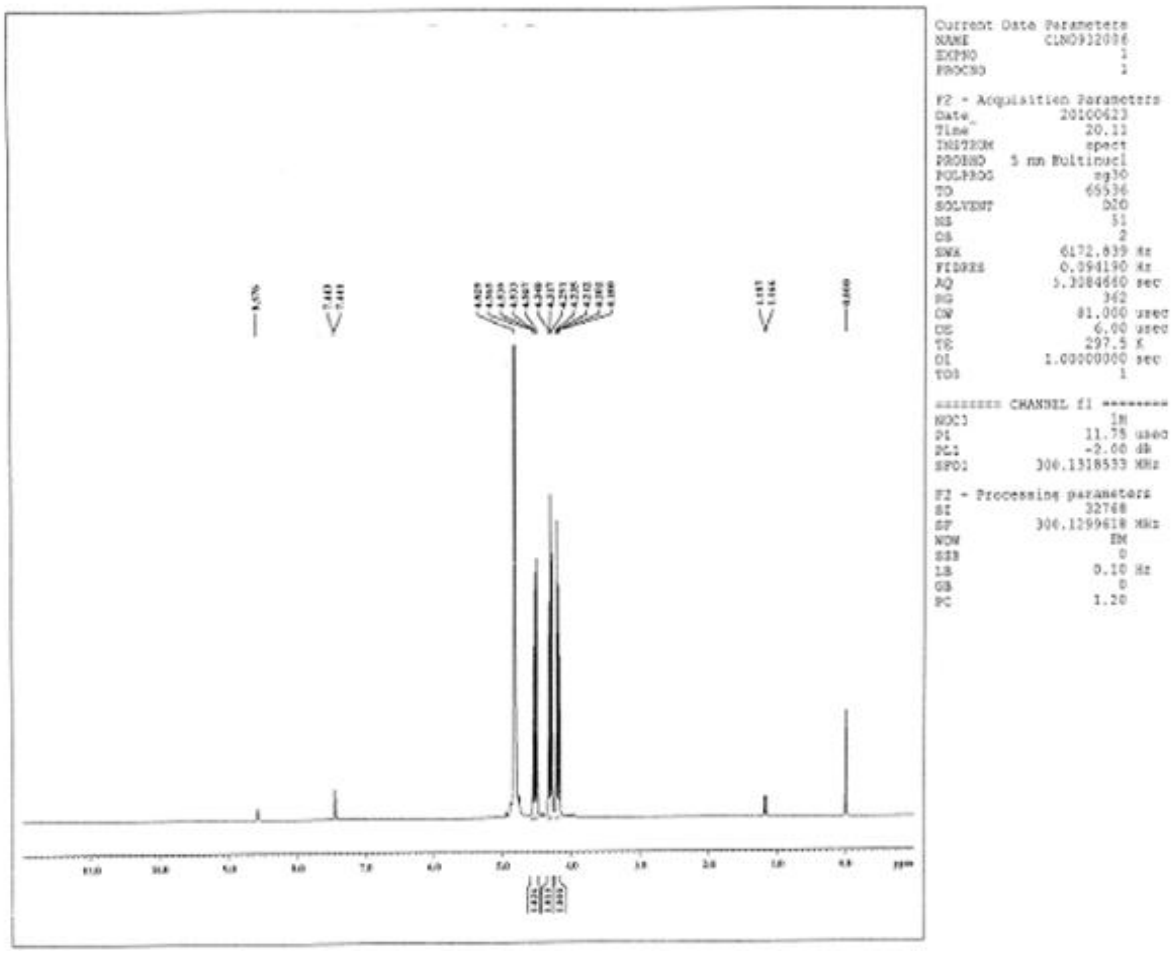

FIGURE: 3.9.3 1H NMR spectrum of cycloserine

the easily exchangeable acidic protons on the N-atoms present in the analyte and it can obscure the observable peaks of these proton from the1H NMR spectrum of the analyte. Like, Deuterated methanol (CD3OH), D2O can also exchange all acidic protons readily and exhibits a strong H-OD signal at 4.9 – 4.7 ppm.

Furthermore, the computed Proton NMR spectrum, **Figure 3.9.4**, of the title compound showed a very good agreement with the observed experimental spectral data.

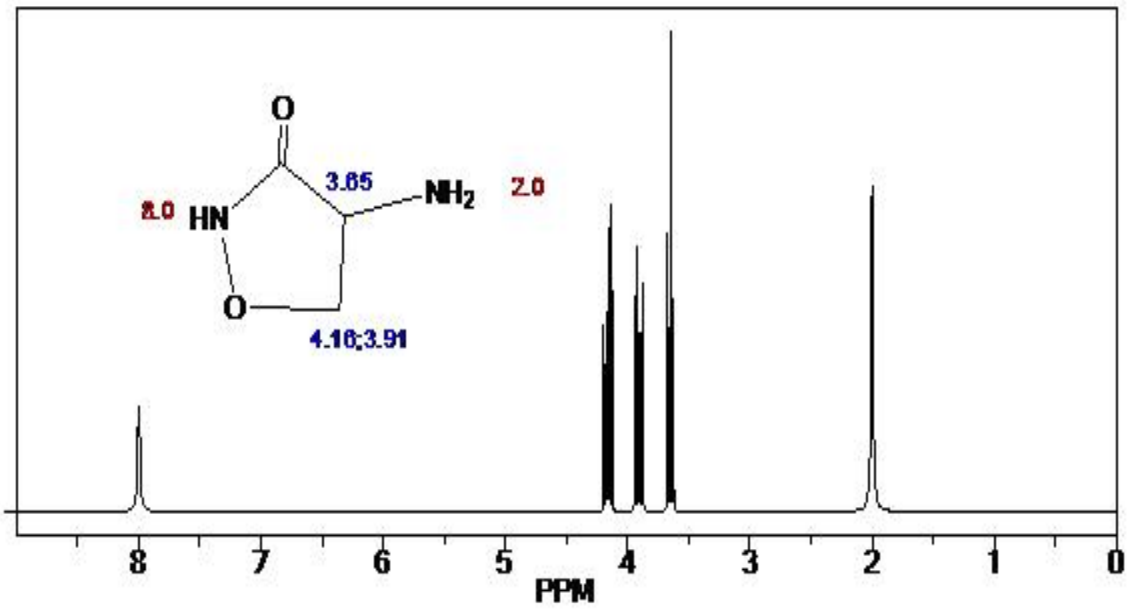

FIGURE: 3.9.4 Simulated 1H NMR spectrum of cycloserine

3.5 13CNMR SPECTRUM OF CYCLOSERINE

The obtained experimental data and spectrum were shown in the **Table 3.9** and in the **Figure 3.9.5** ,

Position	δ-Value (ppm)
1,2	-
3	174.1
4	57.8
5	73.8

13C NMR spectrum displayed two sets of peak in which one appeared in the much downfield region and the rest appeared in the upfield region with respect to the standard reference. Furthermore, the proton decoupled spectrum of the analyte was very well and clearly devoid of any complexity aroused due to the coupling of protons.The peaks at 174.1, 57.8 and 73.8 ppm corresponds to the sp2 hybridized C-atom of the carbonyl function, the sp3 hybridized C-atoms at position-4 and -5 respectively. The radio-frequency absorbance at 174.1 ppm clearly revealed the sp2 hybridized carbonyl C-atom which could be present as an amidic moiety in the analyte. Similarly, the peak at 73.8 ppm, became slightly shifted downfield from a typical sp3 hybridized C-atom of –CH3 group, was more likely corresponds to the sp3 hybridized C-atom which could be bounded to an electronegative atom/substituent which in turn accounted for the downfield shift of **δ-value.**

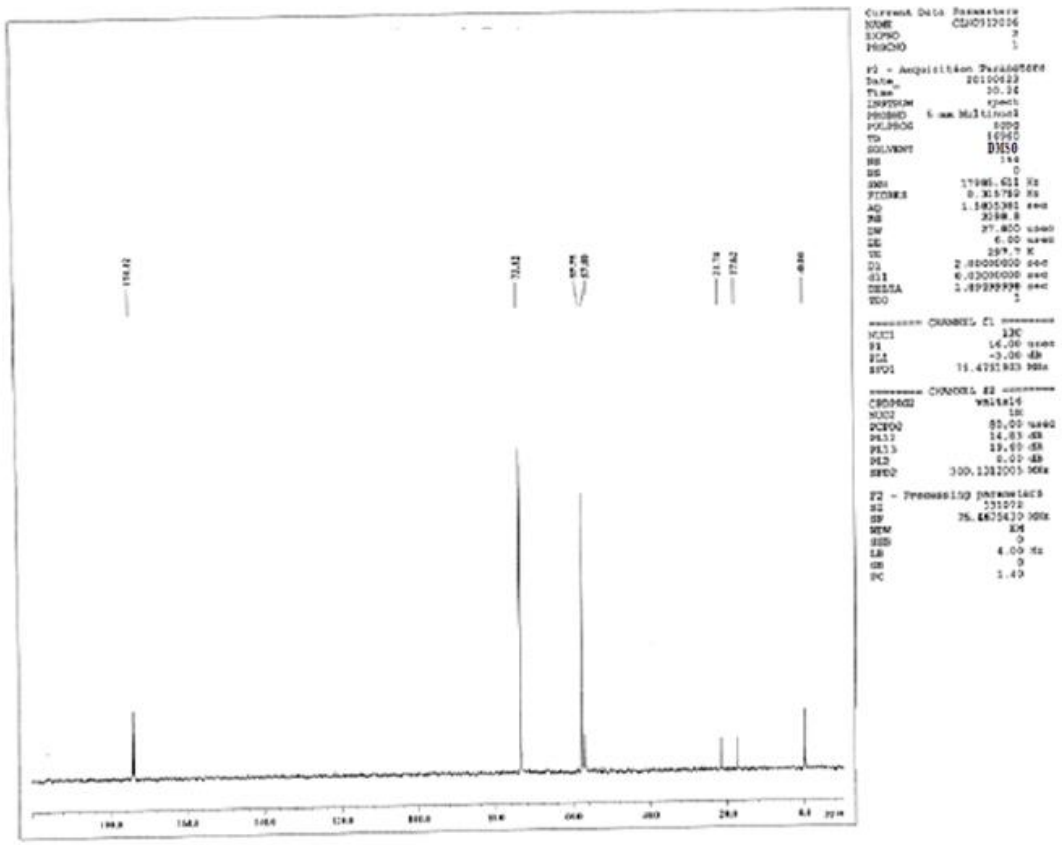

FIGURE: 3.9.5 13C NMR spectrum of cycloserine

The computed **13C** NMR spectrum, **Figure 3.9.6**, of the title compound showed a very good agreement with the observed experimental spectral data.

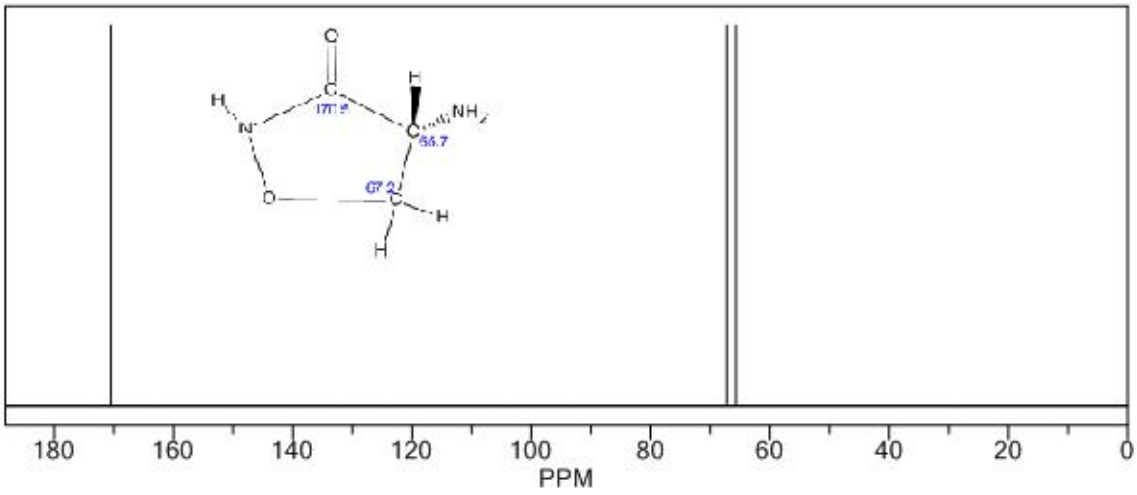

FIGURE: 3.9.6 The computed 13C NMR spectrum of cycloserine

The peak at 57.8 ppm was typically due to sp3 hybridized C-atom with an substituent, most probably –NH2 group, which could be effect the de-shielding of C-atom to a downfield region for about ~30 ppm from its original region. And the peaks between 17-20 ppm correspond to the C-atoms of the methyl groups present in the solvent molecules, CH3-O-CD3, facilitated by an isotopic-exchange reaction between the solvent molecule (DMSO) and the labile acidic protons of the analyte.

With these arguments, it has been concluded that the appearance of peaks at 174.1, 73.8 and 57.8 ppm corresponds to the C-atoms of amide, -CH-NH2 and ≡C-O- moieties at positions 3,4 and 5 respectively.

3.6 HIGH-PERFOMANCE LIQUID CHROMATOGRAPHY

A typical HPLC chromatogram is a plot of milli absorbance unit (mAu) or/ Absorbance unit (Au) versus the retention time of the analyte and the obtained experimental chromatogram of Cycloserine is shown in the **Figure 3.9.7**.

The sharp and intense peak in the chromatogram at 5.1 minutes clearly showed the purity of the analyte, up to 99.9% assay, and a very neat base line of the chromatogram indicates the presence of negligibly very low quantities of impurities in the sample.

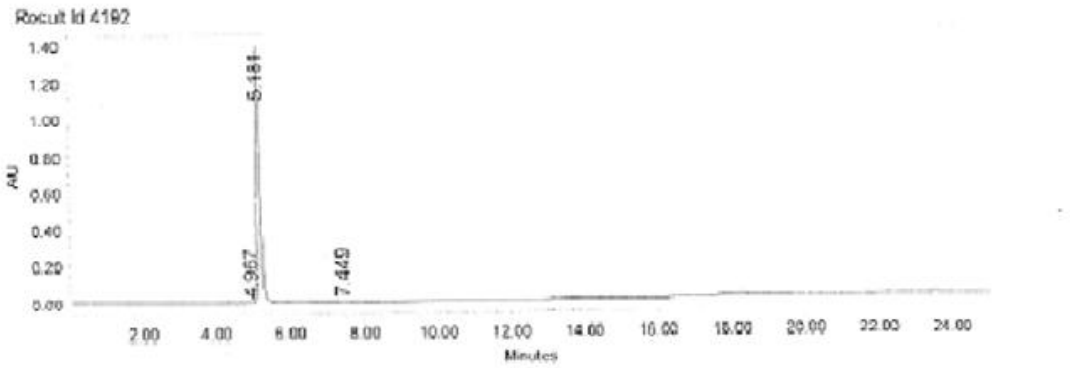

FIGURE 3.9.7 : Achiral (RS) - HPLC chromatogram of cycloserine

It should be noted that the analyte molecule exhibits as a chiral enantiomers of two forms (R) and (S), becomes indistinguishable in the achiral HPLC techniques. However, the peak area integration of the chromatogram will provide sufficient information about the quantity of the impurities and analyte present in the sample and it is shown in the **Table.3.9.0**

TABLE: 3.9.0 HPLC data of cycloserine

	Retention time (min)	Area (µV* sec)	% Area	Name
1	4.97	3375	0.04	-
2	5.18	8829932	99.91	Cycloserine
3	7.45	4810	0.05	-
Sum		8838117		

4. CONCLUSION

Theoretical and experimental values from spectral and computation predicts the unusual structure and drug activity, The angle strain and chiral activity be useful for its drug activity in concluded.

REFERENCES

[1] Prosse; Goreth; de Carvalho; S Luiz Pedro. FEBS Journal, **2013,** 280(4), 1150-1166

[2] Kuehl; A Prederick Jr; J Frank Wolf; R Nelson Terner; L Robert Peck; P Rudolf Buhs; Irvin Putter; Robert Ormond; E John Lyons; Louis Chaiet; Eugene Home; P Berl Hunnewell; Geo Downing; E.L. Newstead; Karl Follers. Journal of American chemical society, **1955,** 77, 2344-2345

[3] Filippi Antonello; Fraschetti Caterina; Grandinetti Felice; Speranza Maurizio; Ponzi Aurora; Decleva Piero; Stranges Stefano. Physical chemical chemical physics, **2015,** 17(39), 25845-25853

[4] A C Weltman; D N Rose. Archive of internal medicine , **1994**, 154(19), 2161-2167

[5] Krueger-Thiemer; Ekkehard; K H Spitzy. Int.congr,chemotherr.,proc.,5th. **1967**, 6, 445-448

[6] Marawan Ahmed; Feng Wang; G Robert Acres; C Kevin Prime. Journal of physical chemistry A, 2014, 118(20), 3645-3654

[7] O Bunmi Olantunji; David Rosenfield; Bendetta Monzoni; Georgina Kerbs; Isobel Heyman; Cynthia Turner; Kayoka Isomura; David Mataix-Cols. Depression and anxiety, 2015, 32(12), 935-943.

[8] J T Stewart; G S Yoo. J,Pharm. Sci., 1988, 77, 452-454

[9] M P Lambert. Journal of bacteriology, 1972, 110(3), 978-987
[10] L T Thompson; J R M oskal; J F Disterhoff. Nature (London), 1992, 359, 638-641
[11] M J Frisch; G W Trucks; H B Schlegel; M A Robb; J R Cheeseman; J A Montogomery Jr; T Vrevan; K N Kudin; J C Burant; J M Millam; S S Iyengar; J Tomasi; V Barone; B Mennuci; M Cossi; G Scalmani; N Renga; G A Petersson; H Nakatatsuji; M Hada; M Ehara; K Toyota; R Fukuda; J Hasegawa; M Ishida; T nakajima; Y Honda; O Kitao; H Nakai; M Klene; X Li; J E Knox; H P Hratchian; J B Cross; C Adamo; J Jaramillo; R Gomperts; R E Stratmann; O Yazyev; A J Austin; R Cammi; C Pomelli; J W Ochterski; P Y Ayala; K Morokuma; S Dapprich; A D Daniels; M C Strain; O Farkas; D K Malik; A D Rabuck; K Raghavachari; J B Foresman; J V Ortiz; Q Cui; A G Baboul; S Cliffoed; J Cioslowski; B B Stefanov; G Liu; A Liashenko; P Piskorz; I Komaromi; R L Martin; D J Fox; T Keith; M A Al-Laham; C Y Peng; A Nanayakkara; M Challacombe; P M W Gilli; B Johnson; W Chen; M W Wong; C Gonzalez; J A Pople. Gaussian 03, Revision B 0.3, Gaussian, Inc., Pittsburgh, PA, 2003
[12] A D Becke. J.Chem.Phys., **1993**, 98, 5648
[13] C Lee; W Yang; R G Parr. Phys.Rev. B, **1988** , 37, 785
[14] L J Bellamy. The Infrared spectra of complex molecules, John Wiley, New York, **1975**
[15] N B Colthup; L H Daly; S E Wimberly. Introduction to Infrared and Raman spectroscopy, 2nd edition, Academic press, New York, **1975**
[16] Fox Maye Anne; K James Whitesell. Orgaische chemie: Grudlagen, Mechanismen, Bio organische Anwendengen, Springer, **1995**, 978(3), 249
[17] Hand book of chemistry and physics, 65th edition, CRC press, USA, **2009**
[18] G Herzberg. Infrared and Raman spectra of polyatomic molecules, Van Nostrand Reianhold, New York, **1945**
[19] P J Stephens; F J Devlin; C F Chabalowski; M J Frisch. J. Phys. Chem., **1994**, 98, 11632
[20] A Frish; A B Nelson and A J Holder, Gauss view user manual, Gaussian Inc., Pittsburgh, USA, **2001**
[21] H Phil Hidy; E B Hodge; V Vernon Young; L Roger Hamand; E Homer Starely; A Pohlard; H Boaz; H R Sullivan. Journal of the American chemical society, **1955**, 77, 2345-2346
[22] P Politzer; P R Laurence; K Jayasuriya. Environ. Health Perp., **1985**, 61, 191
[23] P Politzer; P Lane. Struct. Chem., **1990**, 1, 159

Access this Article in Online

Website: www.icrcps.com

Subject: Pharmaceutical Chemistry

Quick Response Code

How to cite this article:
M Manivannan, B Karthikeyan, K Rajeshwaran. (2016). Evidences of drug activity of cycloserine through experimental and simulated theoretical models. Int. J. Curr. Res. Chem. Pharm. Sci. 3(4):33-49.